Available online at www.sciencedirect.com
ScienceDirect
Journal of the European Ceramic Society 27 (2007) 397–403
www.elsevier.com/locate/jeurceramsoc

Mechanical characterization of a polysiloxane-derived SiOC glass

Claude Moysan [a], Ralf Riedel [b,*], Rahul Harshe [b,1], Tanguy Rouxel [a], Franck Augereau [c]

[a] *Laboratoire de Recherche en Mécanique Appliquée de l' Université de Rennes 1, FRE-CNRS 2717 – Bât. 10B – Campus de Beaulieu, 35042 Rennes Cedex, France*
[b] *Institut für Materialwissenschaft, Technische Universität Darmstadt, Petersenstr. 23, D-64287 Darmstadt, Germany*
[c] *LAIN, UMR 5011, Université Montpellier II, Place E. BATAILLON, CC 082, F-34095 Montpellier Cedex, France*

Received 21 September 2005; received in revised form 17 January 2006; accepted 21 January 2006
Available online 10 March 2006

Abstract

Silicon oxycarbide glass with the composition $Si_{1.0}O_{1.6}C_{0.8}$ was synthesized from a commercial polysiloxane by polymer pyrolysis. Dense SiOC samples were obtained by cross linking of the polysiloxane followed by warm pressing to form cylindrical samples and subsequent pyrolysis of the shaped polymer at 1100 °C in Ar. Hardness (H), Young's modulus (E) and Poisson's ratio (ν) of the as-prepared SiOC glass were evaluated from indentation studies and from acoustic microscopy. Indentation studies showed that E depends on the applied load and amounts to 90 GPa for low load and to 180 GPa for high load. Average values of 6.4 and 101 GPa were obtained for H and E, respectively, by the Vickers indentation method. Acoustic microscopy analysis yielded values of 96 GPa and 0.11 for E and ν, respectively. Compared to vitreous silica, the Young's modulus of the SiOC glass is about 1.3–1.5 times higher. To the knowledge of the present authors, the measured Poisson's ratio ($\nu = 0.11$) is the lowest reported so far for glasses and polycrystalline ceramics.

Keywords: Precursors-organic; Mechanical properties; Glass; Poisson's ratio; SiOC

1. Introduction

Silicon oxycarbide glasses and ceramics are accessible via the polymer pyrolysis technique. Suitable preceramic polymers to produce SiOC are poly(organosiloxanes) and poly(organosilsesquioxanes) of the general composition $[RR'SiO]_n$ and $[RSiO_{1.5}]_n$, respectively where R and R′ = H, methyl, vinyl, phenyl, OH, OEt, etc. Synthesis of SiOC by conventional solid state reactions using SiO_2, SiC and C or Si as starting materials is not possible for thermodynamic reasons.

In the last decade a variety of silicon-based preceramic polymers such as polysilazanes or polysiloxanes were further developed and commercialized. While polysilazanes are still expensive precursors and pose problems in handling as they are sensitive to ambient atmosphere, polysiloxanes are available easily and are cheap in cost and can be converted to silicon oxycarbide (SiOC) ceramic by a thermal treatment (pyrolysis).[1,2] Poly(organosiloxanes) can be handled in air and are available in both liquid, semi-solid (viscous) as well as solid (powder) form. Among all available polymers a proper selection should be done which satisfies the required processing properties. For example, if the polymer is in the liquid state at room temperature it can be easily injected into a mould cavity to form a component but as soon as it reaches the cavity it has to be to cross-linked in order to retain the mould shape. Cross linking can be done thermally via hydrosilylation of vinyl groups containing polymers[3] or via polycondensation reaction.[4] In the case the preceramic polymer itself is a solid material it must be initially meltable and should be prone to cross linking.[5]

In recent years, SiOC based glasses and ceramics have been investigated in more detail in terms of their high temperature stability.[2,6,7] Silicon oxycarbide-based materials containing a variety of fillers are presently commercialized as ceramic heaters or as materials for heat protection of glass fiber fabrics against flame burn through.[8a,b] By the addition of filler particles such as alumina, silicon carbide or metals the mechanical and physical properties of the SiOC matrix can be adjusted over a broad range.[9] However, only few papers reported on the quantitative analysis of the mechanical properties of this new class of mate-

* Corresponding author.
[1] Present address: R&DE(E), Alandi Road, Dighi, Pune 411015, India.

0955-2219/$ – see front matter © 2006 Elsevier Ltd. All rights reserved.
doi:10.1016/j.jeurceramsoc.2006.01.016

rials that resist crystallization up to at least 1300 °C (see for example refs.[6,7]).

The present research is hence focused on the detailed analysis of the Young's modulus and the Poisson's ratio of pure SiOC matrix-derived from a commercial polysiloxane. Our studies first required the synthesis of SiOC bulk materials before we could analyse the mechanical properties. Therefore, the processing of the polymer to dense SiOC bulk samples is an important step in this work and is described in detail in Section 2.

2. Experimental

2.1. Synthesis of SiOC ceramics

Dense SiOC ceramics were obtained from a commercial polysiloxane as reported in refs.[2,5] The polymer used for this research is a product from Wacker Chemie GmbH, Burghausen, with the trade name Wacker-Bensil PMS MK (MK polymer). The MK polymer is a solid solvent free poly(methylsilsesquioxane) polymer with $[CH_3SiO_{1.5}]_n$ basic structure and falls under the silicone resin group. The odorless, colorless flakes of MK-polymer have a softening range between 45 and 60 °C and a good solubility in organic solvents, namely, aromatic solvents and ketones. The polymer possesses approximately 2 mol.% hydroxy and ethoxy groups, as functional units. Accordingly, the possible structure of the used resin along with its functional groups is illustrated in Fig. 1. With evolution of water and ethanol by polycondensation reaction, the formation of a three dimensional network with Si–O–Si alternating units as the backbone takes place. In order to achieve an acceptable process regime, the addition of a suitable cross linking agent in sufficient amount and a distinct thermal treatment are necessary. Zirconium acetylacetonate, $C_{20}H_{28}O_8Zr$, with an amount of 1 wt.% related to the polymer mass was used as cross linking agent (henceforth referred as CLA).

The polysiloxane MK was dissolved in isopropanol along with 1 wt.% CLA and the solution was stirred by a magnetic stirrer for 30 min. The CLA added polymer solution was dried under vacuum at moderate temperature (40–50 °C). The resulting powder was in a semi-dried condition, containing some bigger particles with entrapped solvent. Therefore, the mixture was milled using a ball mill followed by redrying in vacuum for 3–5 h, and subsequently sieved from 100 μm mesh producing free flowing powder. This method resulted in a homogeneous distribution of the CLA in the polymer mass. Shaping of the powder mixture together with cross-linking of the poly(methylsilsesquioxane) to an infusible polymer mass with a three dimensional network of polymer chains is achieved by warm pressing under pressure and high temperature in a metallic die. For warm pressing, a cylindrical steel die with 10 mm internal diameter was used. Around the steel die a heating element was attached, which could operate between ambient temperature and 500 °C. The temperature control was made by a thermocouple, which by an appropriate drilling at half the height of the cylinder is directly positioned beside the pressed powder. Pressure was applied with an oil hydraulic press (Model from Paul–Otto–Weber GmbH) with a maximum load of 100 kN. Before every pressing process, the inner side of the warm pressing form and the used side of the stamps were coated with silicone oil as a lubricant. The use of silicone oil was necessary to reduce the friction between the green body and the pressing form, which otherwise would have caused demoulding difficulty and may have resulted in cracking of the polymeric green body.

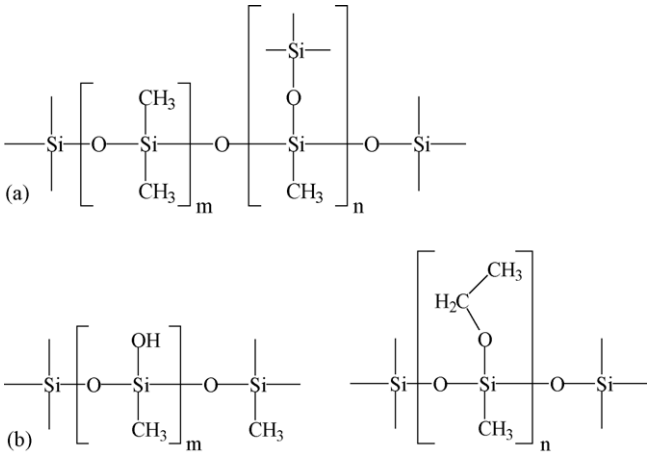

Fig. 1. Section of the molecular structure of the commercial poly(methylsilsesquioxane) Wacker-Bensil PMS MK: (a) linear and crosslinked polymer network units; (b) structural units containing OH- and OEt-functional groups which are used for cross-linking.

In our case, the initial weight of the polymer powder mixture filled in the mould cavity varied between 0.5 and 1 g. The filled pressing die was inserted into the press and heated up with a constant load (4.8 kN for 10 mm diameter form, corresponding to 50 MPa) to the selected warm pressing temperature (150–170 °C). In addition, for all attempts a constant heating rate of 10 °C/min was selected. During the heating cycle, continuous decrease of the applied load was observed between 60 and 110 °C and the load rose with further heating, but was constantly corrected by manual readjustment to the desired value. The compression pressure was maintained for 10–15 min after reaching the final temperature. The pressure was gradually reduced to zero during the cooling cycle and when the temperature reached 100 °C the green body was ejected. Gradual reduction in the applied pressure in the cooling cycle and ejection of the sample at a temperature beyond room temperature avoided damage of the sample. Ejecting the sample at room temperature could lead to crack formation because of the brittle nature of the cross-linked green body. Before pyrolysis the thick green body was sliced by diamond wire saw for maximum thickness of 0.6–0.8 mm.

Pyrolysis of the shaped and cross-linked polymer was accomplished in a quartz tube ($h = 50$ cm, diameter = 3 cm). The green bodies were heated to 1100 °C at a rate of 25 °C/h, held at this temperature for 2 h, and then cooled to room temperature at a rate of 100 °C/h. Due to such long duration of pyrolysis cycle, and in order to avoid oxygen contamination, the top lid of the quartz tube was sealed using high temperature grease (Apiezon H). The quartz tube was inserted perpendicularly in an electrically heated vertical Al_2O_3 tube furnace. The samples were positioned in the correct height of the furnace where the adjusted temperature was reached. This position was frequently calibrated by

an external temperature controller. The lower end of the furnace was closed in order to prevent variations in temperature by radiation. Pyrolysis took place under a constant argon stream via plastic/rubber tubing, which was connected to a flow controller. The applied argon stream provided easy and continuous transport of the decomposition gases out of the quartz tube. The volatile decomposition products along with the used argon were passed through two exhaust bottles partially filled with glycerine. This procedure prevents any access of air in the reverse direction back into the quartz tube. The samples were removed from the quartz tube after ensuring complete cooling of the tube down to room temperature.

2.2. Mechanical properties

Vickers hardness and Young's modulus were evaluated by indentation method. In addition, longitudinal (Young's) and shear elastic moduli as well as Poisson's ratio were evaluated by means of a non-destructive acoustic microscopy method. A detailed description of this method is given below.

2.2.1. Indentation experiments

The indentation behaviour was investigated using a Vickers diamond indenter with the load ranging between 0.098 and 9.81 N and a loading time of 20 s. Most experiments were conducted with a load of 0.098 N to avoid any microcracking with the aim to get rheological parameters from the analysis of the indentation profiles by atomic force microscopy (AFM Nanoscope III, Digital Instruments). All the characteristics were averaged over measurements on three indentations per load value. Error bars on the experimental points mainly derived from the scattering of the AFM measurements. Specimen surfaces were mirror-polished with diamond suspension down to 0.25 μm particle size prior to indentation. Note also that all measurements were performed in a thermally regulated room, at 20 °C. Meyer's hardness (H) is defined by:

$$H = \frac{P}{2a^2} \tag{1}$$

where P (N) is the load applied on the Vickers indenter and a (m) is the half of the mean size of the two diagonals. When elastic recovery is assumed to have little effect on the projected dimension of the indent, Meyer's hardness can be considered as the true hardness, defined as the mean normal stress over the contact region, and is thus a more fundamental measure of hardness than the Vickers' one. The indentation profile could be studied by atomic force microscopy (AFM) as long as the indentation size remained smaller than 50 μm in diagonal length, i.e. provided that the load is smaller than 1 kg. The permanent (u_p), total (u_t) and reversible (u_e) displacement components were systematically estimated from the profiles following the procedure illustrated by the schematic drawing in Fig. 2. The permanent displacement was directly measured on the AFM (or confocal microscope) profile, whereas the total displacement was evaluated by extrapolation, by considering the ideal identation shape at maximum load from the Vickers diamond shape. Then the reversible component, u_e, was deduced: $u_e = u_t - u_p$.

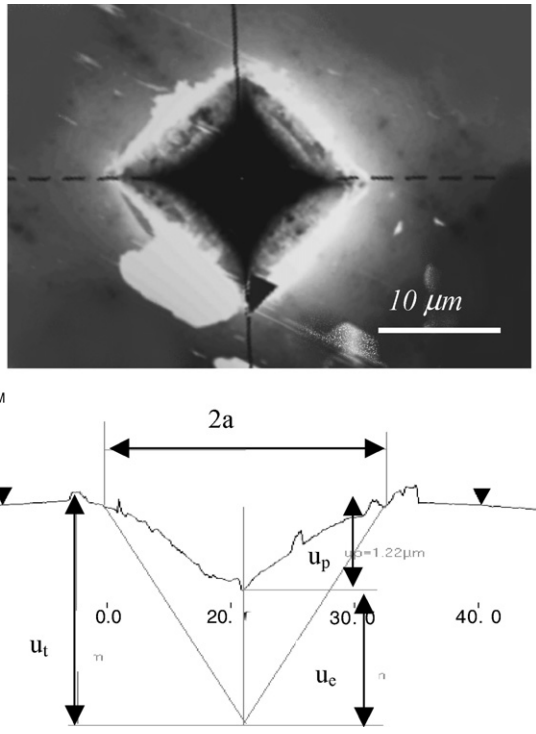

Fig. 2. Typical indentation profile with the different displacement components as measured by AFM (300 g, 30 s).

2.2.2. Acoustic microscopy

The linear elasticity theory makes it possible to give analytical expressions for the propagation velocity of acoustic waves in infinite media (continuum). For instance, E and ν are expressed as follows:

$$E = \rho \frac{3V_l^2 - 4V_t^2}{(V_l/V_t)^2 - 1} \tag{2}$$

$$\nu = \rho \frac{3V_l^2 - 4V_t^2}{2(V_l^2 - V_t^2)} - 1 \tag{3}$$

where ρ is the density of the material, V_l and V_t are the longitudinal and transversal wave velocities, respectively.

The density was measured at 20 °C by the Archimedean displacement technique using CCl_4. The relative error on the density is ±0.5%: $\rho = 2.23\ g/cm^3$.

When the specimen thickness is small, the piezoelectric transverse transducers are often unable to efficiently promote the propagation of shear waves through the specimen. In this latter case, surface-type waves, also called Rayleigh waves, can be used. These waves are characterized by a velocity, V_R, proportional to V_t: $V_R = \zeta V_t$, where ζ is a function of Poisson's ratio, or of the V_l/V_t ratio. V_R and V_l were measured and V_t was optimised to satisfy the following Eq. (4):

$$V_R = \frac{V_t(0.715 - (V_t/V_l)^2)}{0.750 - (V_t/V_l)^2}. \tag{4}$$

3. Results and discussion

Silicon oxycarbide is referred as black glass and is synthesized from poly(organosiloxanes) via polymer-to-ceramic transformation.[1] Compared to vitreous silica, part of the oxygen is substituted by carbon in SiOC glasses. In consequence, the silicon atoms in SiOC glasses are coordinated not only by oxygen but also by carbon. Thus, the typical microstructure of SiOC is characterized by the presence of different Si-tetrahedra ranging from SiO_4 via SiO_3C and SiO_2C_2 to SiC_4 as has been confirmed by solid state ^{29}Si-NMR spectroscopy.[10,11] According to the work reported by Renlund et al. in 1991, the Vicker's hardness H_V, E-modulus and transformation temperature T_g are significantly increased from 6–7 GPa, 70 GPa and 1190 °C for silica to 8–9 GPa, 98 GPa and 1350 °C for SiOC, respectively.[1] The enhanced values are discussed in terms of the Si–C bonds in addition to the Si–O present in SiOC. The carbon content in SiOC varies and depends on the chemical composition of the starting poly(organosiloxane). Thus, the organic substituent attached to the silicon atoms (see Fig. 1) influences the final carbon content of the pyrolysed polymer. In addition, SiOC glasses are not stoichiometric in terms of thermodynamically stable SiO_2 and SiC and contain either excess silicon or excess carbon.[12] In the course of our work, the product as-synthesized at 1100 °C in Ar is black and X-ray amorphous and the chemical composition of the SiOC glass-derived from the MK polymer is analysed to be $Si_{1.0}O_{1.6}C_{0.8}$.[2,5] Assuming that all oxygen is bonded to Si and the remaining Si is bonded to carbon, the following composition with respect to the thermodynamically stable products is derived: 0.8 SiO_2 + 0.2 SiC + 0.6 C. Accordingly, the material contains a significant amount of free carbon that is not bonded to silicon.

In the following, we report on Young's modulus and Poisson's ratio of dense SiOC glass as measured by indentation and by acoustic microscopy. The analysed density of $\rho = 2.23$ g/cm^3 corresponds to that published for silicon oxycarbide, e.g. by Renlund et al.[1]

3.1. Indentation

The SiOC glass specimen exhibits a remarkable resistance against indentation cracking. Cracks usually do not appear at loads lower than 196.2 N (20 kg) (Fig. 3). By comparison, a standard window glass exhibits radial cracks at loads beyond 100 g and vitreous silica exhibits ring-type cracks (intersection of cone cracks with the surface) at a load exceeding 50 g.

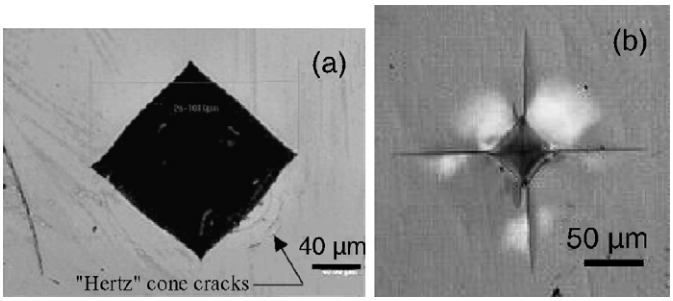

Fig. 3. Vickers indentation: (a) SiOC glass, 20 kg, 20 s (confocal miscroscope); (b) window glass, 1 kg, 20 s (optical microscope).

If cracks tend to form, they show up as surface ring-type cracks, as visible on the bottom right side of the indentation in Fig. 3a. This finding suggests a behaviour resembling the one of vitreous silica. The indentation profile as studied by atomic force microscopy (AFM) is shown in Fig. 2 and the corresponding results are summarized in Table 1.

It is in principle possible to evaluate Young's modulus, E, from the indentation topometry analysis. Lawn et al.[13] and Loubet et al.[14] proposed different methods leading to approximate solutions. In the first approach, a permanent Vickers indentation being loaded elastically from its actual state (deformed material) is assumed to behave as if the material was already pre-stressed, with a pre-stress scaling with the indentation depth (to the power 2), so that the total penetration depth (u_t) comes into play in the equation for E to account for the pre-stress acting along the elastic recovery path:

$$E_{\text{L.H.}} = \gamma^2 \frac{(1-\nu^2)P}{\tan\varphi(2u - u_e)u_e} \tag{5}$$

where subscript (L.H.) refers to the authors of ref.[13] and where φ is half the value of the apical angle of the indenter and, in the present case, is taken as the apical angle of an equivalent cone leading to the same contact pressure for a given penetration depth, i.e. by writing that $\pi R^2 = 2a^2$, where R and a are the radius and half the diagonal of the projected contact area of the conical and Vickers indentations, respectively (see Fig. 4). For the Vickers diamond indenter (148.1° between opposite pyramidal edges), this procedure results in an equivalent cone having an apical angle of 70.3°. Note that the glass is much less rigid than the diamond indenter, so that the latter is assumed to be perfectly rigid.

A major difficulty with the use of Eq. (5) arises from the determination of parameter γ, the relative penetration depth,

Table 1
AFM (columns 2–5) and confocal microscope measurements (columns 6–9) from Vickers indentations performed at loads ranging from 10 to 1000 g

M (g)	$2a$ (µm)	u_t (µm)	u_p (µm)	u_e (µm)	$2a$ (µm)	u_t (µm)	u_p (µm)	u_e (µm)
1000	39.54	5.65	2.40	3.25	39.92	5.70	1.53	4.17
500	37.03	5.29	1.84	3.45	36.57	5.22	1.25	3.97
300	23.91	3.42	1.22	2.20	24.57	3.51	0.18	3.33
50	12.26	1.75	0.92	0.83	11.33	1.62	0.43	1.19
25	9.40	1.34	0.61	0.73	8.98	1.28	0.06	1.22
10	5.67	0.81	0.30	0.51	6.22	0.89	0.03	0.86

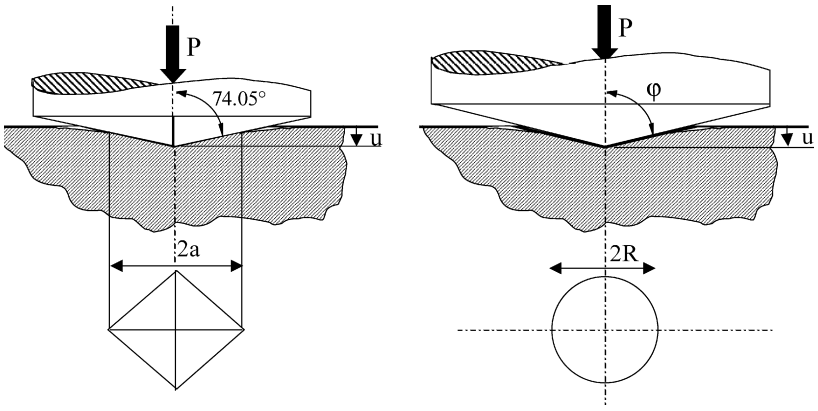

Fig. 4. Vickers indenter (left) with its equivalent cone indenter (right) producing the same contact area for a given penetration depth.

which is introduced to account for the fact that the penetration depth (u) may greatly differ from the contact depth (u_c) (Fig. 5):

$$g = \frac{u}{u_c}. \tag{6}$$

In the case of a perfect linear elastic material γ should be close to $\pi/2$. Nevertheless this may be regarded as an overestimation in real cases, where the behavior is obviously not purely elastic. For instance a value of 0.91 was proposed by Lawn et al.[13] to get a good correlation between experiments and theory in the case of indentation experiments conducted with different materials, including a standard soda–lime–silica glass. It is noteworthy, that in this latter reference focussing on Vickers indentations, the equivalent cone angle was taken equal to 74.05°, i.e. equal to the angle between opposite pyramidal edges. A γ value of about 0.73 would be obtained from their analysis taking an equivalent angle of 70.3°.

In the second approach,[14] the elastic displacement originating from Vickers indentation is assimilated to the one which would be produced by a flat cylindrical punch under the same load provided that the contact area is identical to the one of the Vickers indenter contact. The elastic solution obtained by Sneddon[15] for a flat punch hence applies to the problem and the following equation is finally derived:

$$E_{\text{L.S.}} = \frac{\gamma^2}{\sqrt{2\pi}} \frac{(1-\nu^2)P}{\tan\varphi u u_e}. \tag{7}$$

In Eqs. (6) and (7), a unique γ parameter was introduced. However, it should be underlined that γ certainly takes considerably different values during the loading and the unloading stages, and may evolve throughout both stages as well. It is noteworthy that to the knowledge of the authors, all previous studies assumed a constant value for γ although it depends much on the mechanical behaviour of the material, being as high as 1.3 when elasticity predominates and as low as 0.8 when the material behaves in an essentially "plastic" manner. According to a previous work reported by Lawn and Howes[13] γ correlates with the Poisson's ratio. Applying Eq. (5), we derived the following intercorrelation: $\gamma = 2.2\nu + 0.53$. In our study, a value of 0.11 was evaluated by acoustic microscopy for ν, so that γ was determined to be 0.77. Fig. 6 shows the Young's modulus calculated according to Eq. (5) (see also ref.[16]) as a function of the indentation load.

Young's modulus ranges between 90 (low load) and 180 GPa (high load). The load effect is possibly linked to the flow densification process which occurs in the SiOC glass as well as in vitreous silica, and results in a harder and stiffer material beneath the indenter. It is important to note also that high loads enhance the occurrence of microcracks which may affect the result by reducing the amount of energy available to deform

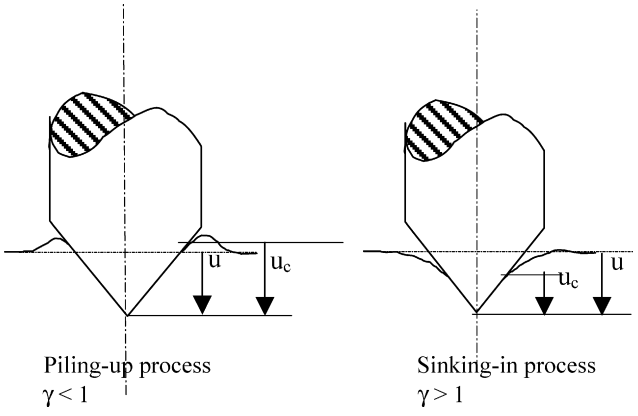

Fig. 5. Schematic drawing of the piling-up and sinking-in phenomena occurring during indentation with a conical or a pyramidal indenter.[16]

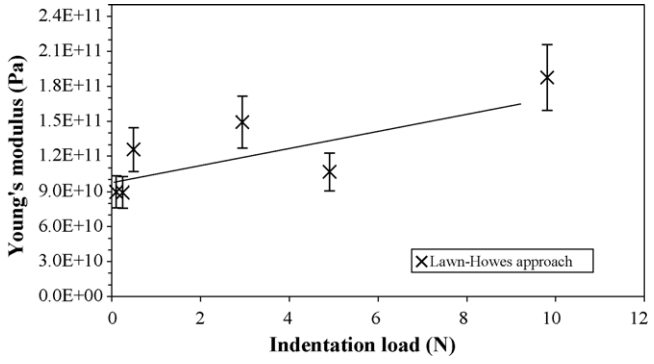

Fig. 6. Young's modulus as calculated by means of Eq. (5) as a function of the indentation load.

the material, so that both H and E are expected to increase at high loads. Average hardness and Young's modulus of 6.4 ± 1 and 101 ± 15 GPa, respectively, were estimated from the experimental data obtained for indentation loads lower than 100 g.

It should be mentioned that the commonly used continuous indentation stiffness method is inadequate to evaluate the elastic properties of the SiOC glass since it was observed that flow densification contributes to the indentation deformation which changes the local stiffness and invalidates the standard equation used to estimate E from the slope during the unloading stage.

3.2. Acoustic microscopy

The surface wave velocity V_l, V_R and V_t were measured along a radius at the surface of a SiOC disk, on both sides. The values for V_R as well as the corresponding calculated E moduli are shown in Fig. 7a and b. A gradient was observed from the surface to the centre, especially in a 2 mm thick ring including the surface. Furthermore, properties were slightly different from one side to another. In a region showing homogeneous colour and located within 2 mm from the specimen centre, E and ν values of 96.1 ± 0.5 GPa and 0.11 ± 0.02 were determined, respectively. These measured value gradients are likely to correlate with chemical gradients. The different chemical composition between core and rim in cylindrical polymer-derived bulk samples is due to the complex decomposition mechanism of compacted polymer powders and has been discussed and reported for example in ref.[17] One essential point is that the partial pressures of the evolved pyrolysis gases like H_2 and CH_4 vary between the surface and the centre of the material during polymer pyrolysis generating chemical heterogeneities.

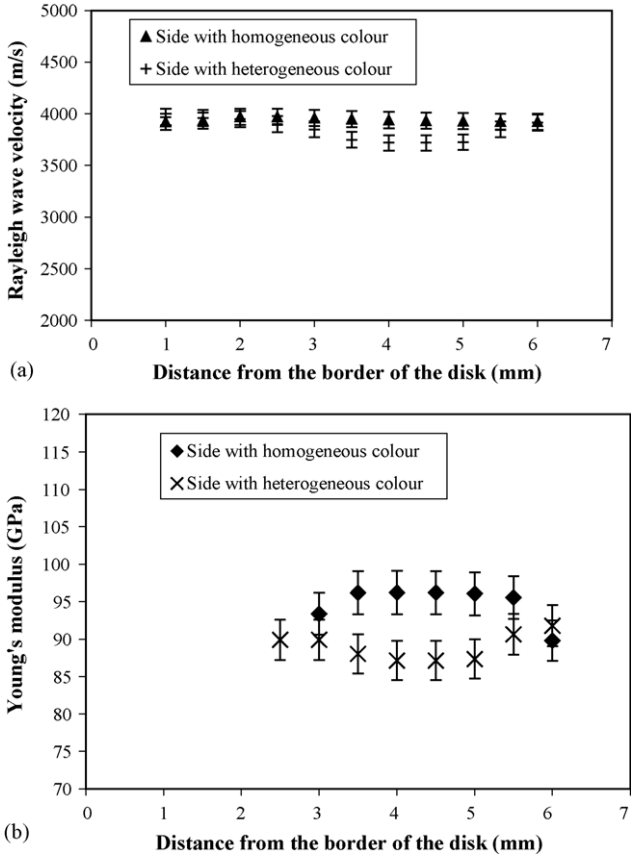

Fig. 7. (a) Rayleigh wave velocity; (b) Young's modulus (from Eq. (5)).

The Young's modulus analysed in this study is in the range of SiOC glass obtained from polysiloxanes with the composition $D_HT_H0.5$ ($E = 104$ GPa) and D_HT_H1 ($E = 110$ GPa) as reported by Soraru et al.[18] The measured Poisson's ratio $\nu = 0.11$ is significantly lower than that for other ceramics and glasses and is, to our knowledge, the lowest Poisson's ratio in this class of materials known so far. Most materials show values between 0.2 and 0.4 and vitreous silica is characterized by $\nu = 0.17$. A low Poisson's ratio means that the corresponding material has an enhanced tendency for volume change under mechanical load. On the contrary, a value of $\nu = 0.5$ corresponds to volume conservation.

4. Conclusion and outlook

Silicon oxycarbide glass of the composition $Si_{1.0}O_{1.6}C_{0.8}$ was produced by polymer pyrolysis of a commercial polysiloxane. For mechanical testing, the polymer was processed to give dense cylindric samples by (i) cross-linking of the polysiloxane, (ii) warm pressing of the cross linked material and finally (iii) pyrolysis of the shaped polymer at 1100 °C in Ar.

Hardness, Young's modulus and Poisson's ratio of the obtained dense glass were analyzed. The hardness was determined to be 6.4 GPa and corresponds to that of silica. It was found that E varies from the surface to the interior of the sample between 85 and 96 GPa with increasing modulus in the inner volume of the sample indicating different chemical composition between the outer and inner part of the cylinder. Interestingly, the sample sustained indentation loads up to 20 kg for 20 s without cracking. This behaviour is related to network rearrangement under the indenter resulting in densification. Network densification is also probably responsible for the increase in E with increasing load, starting at 90 GPa for low load and reaching 180 GPa at high load. An average Young's modulus of 101 GPa was derived from indentation studies while 96 GPa was obtained by acoustic microscopy. It is hence concluded that SiOC is significantly stiffer than vitreous silica ($E \approx 73$ GPa). Despite E still being rather low (oxynitride glasses exhibit Young's moduli higher than 150 GPa), SiOC glasses are potential materials with high thermal shock resistance and are suitable for high temperature applications between 1000 and 1300 °C.

The analysed Poisson's ratio $\nu = 0.11$ is exceptionally low and falls below the value of pure silica. The low Poisson's ratio implies a high reversible volume change under mechanical load and is associated to a remarkable ability of the glass to accommodate sharp contact loading deformation without microcracking.

Acknowledgement

R.H. thanks the Federal State of Hessen, Germany, for providing a PhD grant.

References

1. Renlund, G. M. and Prochazka, S., Silicon oxycarbide glasses: Part I. Preparation and chemistry. *J. Mater. Res.*, 1991, **6**, 2716–2722.
2. Harshe, R., Balan, C. and Riedel, R., Amorphous Si(Al)OC ceramic from polysiloxanes: bulk ceramic processing, crystallization behavior and applications. *J. Eur. Ceram. Soc.*, 2004, **24**, 3471–3482.
3. Veith, M., Elsässer, R. and Krüger, R.-P., Synthesis of dendrimers with a N–Si–C framework. *Organometallics*, 1999, **18**, 656–661.
4. Kroke, E., Li, Y.-L., Konetschny, C., Lecomte, E., Fasel, C. and Riedel, R., Review-article: Silazane-derived ceramics and related materials. *Mater. Sci. Eng. R*, 2000, **26**, 97–199.
5. Harshe, R., Synthesis and processing of amorphous Si(Al)OC bulk ceramics: high temperature properties and applications, Ph.D. Thesis, TU Darmstadt, 2004 (see also the electronic publication of the TU Darmstadt at: http://elib.tu-darmstadt.de/diss/000512/.
6. Rouxel, T., Soraru, G.-D. and Vicens, J., Creep viscosity and stress relaxation of gel-derived silicon oxycarbide glasses. *J. Am. Ceram. Soc.*, 2001, **84**, 1052–1058.
7. Rouxel, T., Massouras, G. and Soraru, G.-D., High temperature behavior of a gel-derived SiOC glass: elasticity and viscosity. *J. Sol–Gel Sci. Technol.*, 1999, **14**, 87–94.
8. Personnel information provided by;
   (a) Klonzcynski, A., Robert Bosch GmbH, Stuttgart, Gemany;
   (b) Starfiresystems, USA (see also http://www.starfiresystems.com/).
9. Greil, P., Active-filler-controlled pyrolysis of preceramic polymers. *J. Am. Ceram. Soc.*, 1995, **78**, 835–848.
10. Gervais, C., Babonneau, F., Dallabonna, N. and Soraru, G.-D., Sol–gel-derived silicon-boron oxycarbide glasses containing mixed silicon oxycarbide (SiC_xO_{4-x}) and boron oxycarbide (BC_yO_{3-y}) units. *J. Am. Ceram. Soc.*, 2001, **84**, 2160–2164.
11. Klonczynski, A., Riedel, R., unpublished.
12. Raj, R., Riedel, R. and Soraru, G.-D., Introduction to the special topical issue on ultrahigh-temperature polymer-derived ceramics. *J. Am. Ceram. Soc.*, 2001, **84**, 2158–2159.
13. Lawn, B.-R. and Howes, V.-R., Elastic recovery at hardness indentations. *J. Mater. Sci.*, 1981, **16**, 2745–2752.
14. Loubet, J.-L., Georges, J.-M. and Meille, G., Vickers indentation curves of elastoplastic materials. In *Microindentation Techniques in Materials Science and Engineering*, *889*, ed. Blau and Lawn. ASTM-STP, 1984, pp. 73–89.
15. Sneddon, I. N., The relation between load and penetration in the axisymmetric Boussinesq problem for a punch of arbitrary profile. *Int. J. Eng. Sci.*, 1965, **3**, 47–57.
16. Rouxel, T., Sangleboeuf, J.-C., Moysan, C. and Truffin, B., Indentation topometry in glasses by atomic force microscopy. *J. Non-Cryst. Sol.*, 2004, **344**, 26–36.
17. Reschke, S., Haluschka, C., Riedel, R., Lences, Z. and Galusek, D., In situ generated homogeneous and functionally graded ceramic materials derived from polysilazane. *J. Eur. Ceram. Soc.*, 2003, **23**(11), 1963–1970.
18. Soraru, G., Dallapiccola, E. and D'Andrea, G., Mechanical characterization of sol-gel derived silicon oxycarbide glasses. *J. Am. Ceram. Soc.*, 1996, **79**, 2074–2080.